

## Distribution and spatio-temporal biomass trends of red mullets across the Mediterranean

George Tserpes<sup>1</sup>, Enric Massutí<sup>2</sup>, Fabio Fiorentino<sup>3</sup>, Maria Teresa Facchini<sup>4</sup>, Claudio Viva<sup>5</sup>,  
Angélique Jadaud<sup>6</sup>, Aleksandar Joksimovic<sup>7</sup>, Paola Pesci<sup>8</sup>, Corrado Piccinetti<sup>9</sup>,  
Letizia Sion<sup>10</sup>, Ioannis Thasitis<sup>11</sup>, Nedo Vrgoc<sup>12</sup>

<sup>1</sup> Hellenic Centre for Marine Research, Institute of Marine Biological Resources and Inland Waters, PO Box 2214, 71003 Heraklion, Greece.

(GT) (Corresponding author) E-mail: [gtserpes@hcmr.gr](mailto:gtserpes@hcmr.gr). ORCID iD: <https://orcid.org/0000-0001-9052-4091>

<sup>2</sup> Instituto Español de Oceanografía, Centre Oceanogràfic de les Balears, Moll de Ponent s/n, 07015 Palma de Mallorca, Spain.

(EM) E-mail: [enric.massuti@ieo.es](mailto:enric.massuti@ieo.es). ORCID iD: <https://orcid.org/0000-0002-9524-5873>

<sup>3</sup> Italian National Research Council (CNR), Institute for Coastal Marine Environment (IAMC), Mazara del Vallo, Italy.

(FF) E-mail: [fabio.fiorentino@iamc.cnr.it](mailto:fabio.fiorentino@iamc.cnr.it). ORCID iD: <https://orcid.org/0000-0002-6302-649X>

<sup>4</sup> COISPA Tecnologia & Ricerca, Stazione Sperimentale per lo Studio delle Risorse del Mare, Via dei Trulli, 18/20, 70126, BARI Torre a Mare, Italy.

(MTF) E-mail: [facchini@coispa.it](mailto:facchini@coispa.it). ORCID iD: <https://orcid.org/0000-0001-6930-2961>

<sup>5</sup> Centro Interuniversitario di Biologia Marina ed ecologia applicata (CIBM), Livorno, Italy.

(CV) E-mail: [viva@cibm.it](mailto:viva@cibm.it). ORCID iD: <https://orcid.org/0000-0001-6900-3398>

<sup>6</sup> IFREMER-UMR MARBEC, Fisheries Laboratory, Avenue Jean Monnet, CS 30171, 34203 Sète Cedex, France.

(AJa) E-mail: [Angelique.Jadaud@ifremer.fr](mailto:Angelique.Jadaud@ifremer.fr). ORCID iD: <http://orcid.org/0000-0001-6858-3570>

<sup>7</sup> University of Montenegro-Institute of Marine Biology, Dobrota bb, 85 330 Kotor, Montenegro.

(AJo) E-Mail: [acojo@ac.me](mailto:acojo@ac.me). ORCID iD: <https://orcid.org/0000-0002-0796-4641>

<sup>8</sup> Department of Life and Environmental Sciences, University of Cagliari, via T. Fiorelli 1, 09126 Cagliari, Italy.

(PP) E-mail: [ppesci@unica.it](mailto:ppesci@unica.it). ORCID iD: <https://orcid.org/0000-0002-9066-8076>

<sup>9</sup> Laboratorio di Biologia Marina e Pesca, Dip.to BiGEOA, Università di Bologna, viale Adriatico 1/n, 61032 Fano, Italy.

(CP) E-mail: [corrado.piccinetti@unibo.it](mailto:corrado.piccinetti@unibo.it). ORCID iD: <https://orcid.org/0000-0002-4928-4353>

<sup>10</sup> Department of Biology, University of Bari Aldo Moro, Via Orabona 4, 70125 Bari, Italy.

(LS) E-mail: [letizia.sion@uniba.it](mailto:letizia.sion@uniba.it). ORCID iD: <https://orcid.org/0000-0002-0308-1841>

<sup>11</sup> Department of Fisheries and Marine Research, 101 Vithleem str., 1416 Nicosia, Cyprus.

(IT) E-mail: [ithasitis@dfmr.moa.gov.cy](mailto:ithasitis@dfmr.moa.gov.cy). ORCID iD: <https://orcid.org/0000-0002-0940-2212>

<sup>12</sup> Institute of Oceanography and Fisheries, Setaliste Ivana Mestrovica 63, 21000 Split, Croatia.

(NV) E-mail: [vrgoc@izor.hr](mailto:vrgoc@izor.hr). ORCID iD: <https://orcid.org/0000-0002-5208-4512>

**Summary:** The present work examines the spatio-temporal biomass trends of *Mullus barbatus* and *Mullus surmuletus* in the Mediterranean Sea through the analysis of a time series of data coming from the Mediterranean International Trawl Surveys (MEDITS), accomplished annually from 1994 to 2015. The biomass of both species showed clear declining trends below 150 to 200 m depth, which were steeper in the case of *M. barbatus*. Increases in temporal biomass trends were observed for *M. barbatus* from 2008 onward in most geographic sub-areas (GSAs), while stability was mostly observed for *M. surmuletus*. For both species, dynamic factor analysis revealed similarities among neighbouring GSAs and the subsequent cluster analysis identified two major GSA groups corresponding to the eastern and western basins of the Mediterranean. Overall, the results suggested that the combined effects of fishing and environmental conditions determine species abundance variations, but the relative importance of each component may vary among areas.

**Keywords:** red mullet; striped red mullet; distribution; trends; Mediterranean.

### Distribución y tendencias espacio-temporales de la biomasa de salmonetes a lo largo del Mediterráneo

**Resumen:** Este trabajo examina las tendencias espacio-temporales de la biomasa de *Mullus barbatus* y *Mullus surmuletus* en el mar Mediterráneo, a través del análisis de una serie temporal de datos procedentes de las campañas internacionales de arrastre MEDITS en el Mediterráneo, realizadas anualmente entre 1994 y 2015. La biomasa de ambas especies mostró tendencias claramente decrecientes por debajo de 150-200 m de profundidad, que fueron más pronunciadas en el caso de *M. barbatus*. En la mayoría de las Sub-áreas Geográficas (SAGs), se han observado incrementos en las tendencias temporales de la biomasa de *M. barbatus* a partir de 2008, mientras las series de datos de *M. surmuletus* mostraron estabilidad en la mayoría de los casos. Para ambas especies, el análisis factorial dinámico reveló similitudes entre las SAGs vecinas y el posterior análisis de conglomerados identificó dos grupos principales de SAGs, correspondientes a las cuencas oriental y occidental del Mediterráneo. En general, los resultados sugieren que los efectos combinados de la pesca y las condiciones ambientales determinan las variaciones en la abundancia de estas especies, pero la importancia relativa de cada componente puede variar entre las áreas.

**Palabras clave:** salmonete de fango; salmonete de roca; distribución; tendencias; Mediterráneo.

**Citation/Cómo citar este artículo:** Tserpes G., Massuti E., Fiorentino F., Facchini M.T., Viva C., Jadaud A., Joksimovic A., Pesci P., Piccinetti C., Sion L., Thasitis I., Vrgoc N. 2019. Distribution and spatio-temporal biomass trends of red mullets across the Mediterranean. *Sci. Mar.* 83S1: 43-55. <https://doi.org/10.3989/scimar.04888.21A>

**Editor:** M.T. Spedicato.

**Received:** March 3, 2018. **Accepted:** September 20, 2018. **Published:** March 19, 2019.

**Copyright:** © 2019 CSIC. This is an open-access article distributed under the terms of the Creative Commons Attribution 4.0 International (CC BY 4.0) License.

## INTRODUCTION

Red mullet (*Mullus barbatus* L., 1758) and striped red mullet (*Mullus surmuletus* L., 1758) are demersal fish distributed throughout the Mediterranean and Black seas, as well as in the eastern Atlantic, from the North Sea to Senegal (Fischer et al. 1987). They inhabit depths down to 300 to 400 m, with red mullet preferring muddy bottoms, while striped red mullet is generally found in bottoms with heterogeneous granulometry and even in *Posidonia* beds.

Both are species of high commercial value and are the main targets of several Mediterranean demersal fisheries (Farrugio et al. 1993, Relini et al. 1999, Papaconstantinou and Farrugio 2000). Red mullet in particular is one of the most important targets of several bottom-trawl fisheries operating along the continental shelf. It is generally considered that its stocks undergo high fishing pressure, but recent studies suggest that they are in better condition than other commercially exploited demersal species (Vasilakopoulos et al. 2014, Tserpes et al. 2016, Cardinale and Scarcella 2017).

Various studies have examined the distribution of *M. barbatus* and *M. surmuletus* in Mediterranean areas and have commented on their bathymetrical distribution and abundance variations (e.g. Machias et al. 1998, Tserpes et al. 1999, Lombarte et al. 2000). However, the employment of different sampling schemes has not allowed for direct comparisons among areas that could provide a much broader picture of the species distribution. A previous analysis of data coming from the in-

ternational bottom-trawl survey (MEDITS) identified Mediterranean-wide abundance trends for both species for a time period of 7 years (Tserpes et al. 2002). The analysis, however, did not focus on the regional level, so no information regarding similarities/dissimilarities among areas was provided.

In the present work, we analyse a longer series of data from the MEDITS surveys with the aim of identifying biomass trends at the geographical sub-area (GSA; Fig. 1) level established by the General Fisheries Commission for the Mediterranean (GFCM), as well as to detect general patterns prevailing at a larger spatial scale. Our findings are discussed in relation to the fisheries exploitation patterns, the environmental features of the area and the biological characteristics of the species.

## MATERIALS AND METHODS

### Sampling

Data were collected in the framework of the MEDITS bottom-trawl surveys accomplished in the period 1994-2015 at 15 GSAs of the Mediterranean (Fig. 1). Sampling included annual sampling at pre-defined stations following a standardized protocol (see Bertrand et al. 2002, Spedicato et al. 2019). Trawling was performed by means of the experimental net GOC-73 with a 20-mm square mesh cod-end, and selection of stations was based on a depth-stratified sampling scheme that included five depth strata: 10-50, 51-100, 101-200,

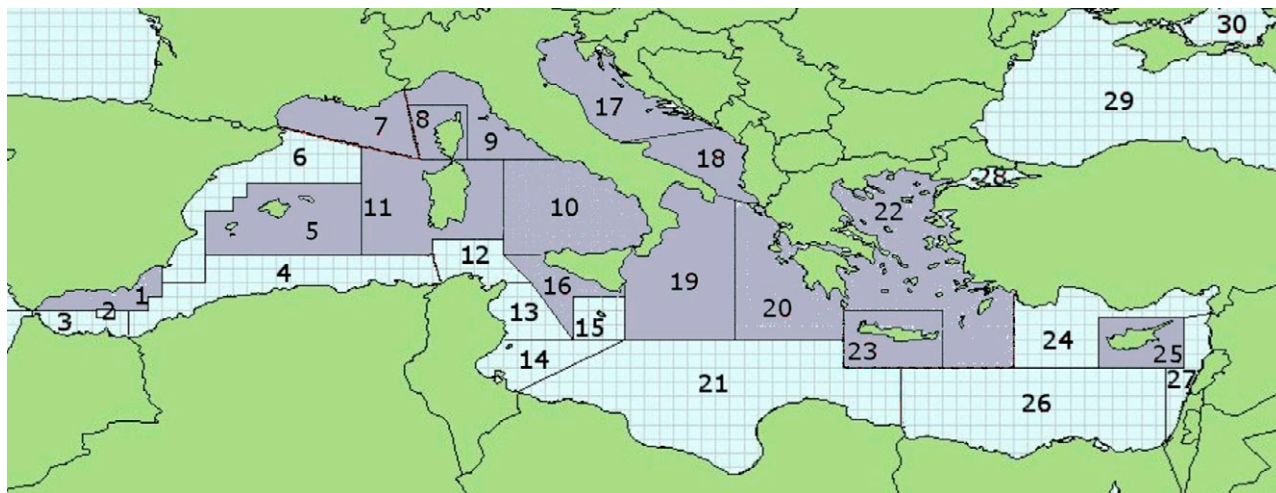


Fig. 1. – Geographical sub-areas of the Mediterranean according to the GFCM. The present study is based on survey data from the 15 shaded areas.

201-500 and 501-800 m. Collected data included number, weight, gonad maturation stage and total length measurements for a wide range of fish, cephalopod and crustacean species. In the present study we analysed biomass data for red and striped red mullets by station, expressed in terms of kg per square km of swept area ( $\text{kg km}^{-2}$ ).

## Data analysis

The analysis utilized generalized additive modelling (GAM) techniques (Hastie and Tibshirani 1990) to investigate the effects of station position and depth on species biomass index. The main advantage of GAM over traditional regression methods is its capability to model non-linear relationships (a common feature of many ecological datasets) between a response variable and multiple explanatory variables using non-parametric smoothers. In the present case, the non-linear predictors included sampling position (entered as the latitude-longitude interaction), depth and year of sampling. A preliminary analysis indicated that the presence of red mullets at depths over 400 m was negligible, so the stations below that depth were not considered in the analysis. The final data set included a total of 16716 hauls.

Given the existence of stations with no presence of red mullets, and based on the diagnostic randomized quantile residual plots (Foster and Branvinton 2013), Tweedie GAM models following a compound Poisson-gamma approach were applied. This avoids multiple-stage modelling of zero-inflated data and allows the probability of presence and the non-zero sampled quantity to be modelled jointly (Shono 2008, Lecomte et al. 2013).

The smoother function used for the year and depth effects was a penalized cubic regression spline and model fitting was accomplished using the mgcv library (Wood 2006) under the R language environment. The procedure automatically selects the degree of smoothing based on the generalized cross-validation score, which is a proxy for the model's predictive performance. However, to avoid dubious relationships, the model was constrained to be at maximum a quartic relationship. Hence, the maximum degrees of freedom for each smoothing term, measured as number of knots (k), was set to 4 (i.e.  $k=5$  in the GAM formulation). For the longitude-latitude interactions the smoother function used was thin plate regression splines, which are low-rank isotropic smoothers without knots, which provide a sensible way of modelling interaction terms, avoiding problems associated with knot placement (Wood 2003). GAM models assumed a log link function and were fitted for each GSA separately. Deficiencies of the fitted models were diagnosed by means of randomized quantile residual plots (Foster and Branvinton 2013).

In the next step, dynamic factor analysis (DFA, Zuur et al. 2003) was applied to the estimated year effects from the GAM models, in order to identify common time series trends among GSAs. The method is based on fitting and comparing models assuming a linear

combination of N common trends that are modelled as smoothing curves by means of a Kalman filter/smoothing algorithm. In the present case, models containing 1 to 3 common trends were tested and the “best” candidate model was defined based on the Akaike information criterion (AIC), which provides a balance between the model fit and the parameters used. The model with the smallest AIC value was selected. Model fit was accomplished under the R language environment using the MARSS library (Holmes et al. 2012). As the data were previously standardized, an “identity” structure for the error covariance matrix R was assumed. Subsequently, hierarchical cluster analysis was used in order to facilitate identification of common GSA groups based on the factor loadings from the common trends estimated from the DFA. The Euclidean distance was used to represent dissimilarity among GSAs and clustering was done using the average linkage method. All statistical inferences were based on the 95% confidence level.

## RESULTS

### *M. barbatus*

The highest values of mean standardized biomass ( $\text{kg km}^{-2}$ ) were observed in Corsica (GSA 8) and Crete (GSA 23) and the lowest ones in the most western areas (Table 1).

The GAM models applied to the biomass indexes explained a large proportion of the total variance (>55% in the majority of the GSAs), while depth and latitude-longitude interactions were always significant. The effect of year was significant in all GSAs apart from 8 and 20 (Supplementary material Table S1). Variations were observed among GSAs regarding the estimated temporal biomass pattern, but in most GSAs of the central and eastern part of the Mediterranean, increasing trends were observed from 2008 onward. A decreasing trend was observed in the Balearic Islands (Fig. 2). Generally, biomass was found to decrease with depth, and this was more evident at depths below 200 m (Fig. 3).

DFA model fitting to the 15 time series was accomplished assuming 1 to 3 common trends (CT). The AIC values for the one-, two- and three-CT models were 668.39, 666.75 and 686.48, respectively. Thus, the

Table 1. – Mean and standard error of biomass index estimates ( $\text{kg km}^{-2}$ ) for *M. barbatus*, by GSA. The last column indicates the number of stations at depths of less than 400 m.

GSA	Mean	Std. error	N
1 - Northern Alboran Sea	18.18	2.34	521
5 - Balearic Island	14.88	3.23	357
7 - Gulf of Lion	13.98	0.87	1288
8 - Corsica	97.33	18.61	304
9 - Ligurian and northern Tyrrhenian Seas	27.36	1.72	2081
10 - Southern and central Tyrrhenian Seas	15.76	1.49	1006
11 - Sardinia	32.91	4.58	1766
16 - Southern Sicily	19.60	1.71	1103
17 - Northern Adriatic Sea	32.42	1.36	3638
18 - Southern Adriatic Sea	13.89	1.19	1709
19 - Western Ionian Sea	33.03	5.87	884
20 - Eastern Ionian Sea	33.90	3.81	316
22 - Aegean Sea	23.92	2.60	1311
23 - Crete	67.62	16.50	217
25 - Cyprus	18.74	3.56	215

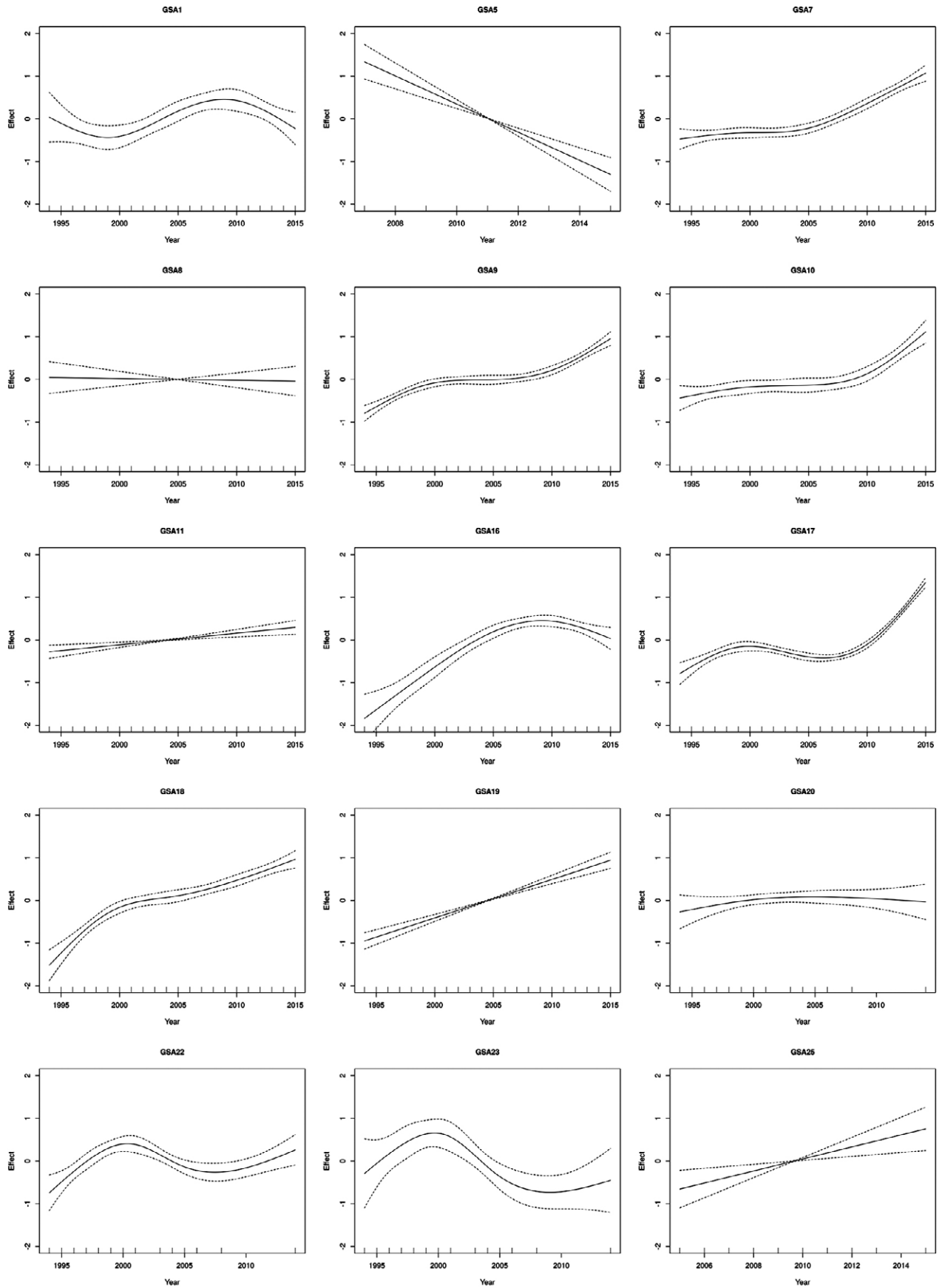


Fig. 2. – GAM derived effect of year on the biomass index ( $\text{kg km}^{-2}$ ) of *M. barbatus*, by GSA. Zero lines indicate mean model estimates and broken lines indicate two standard errors. No statistical significance was found in GSAs 8 and 20.

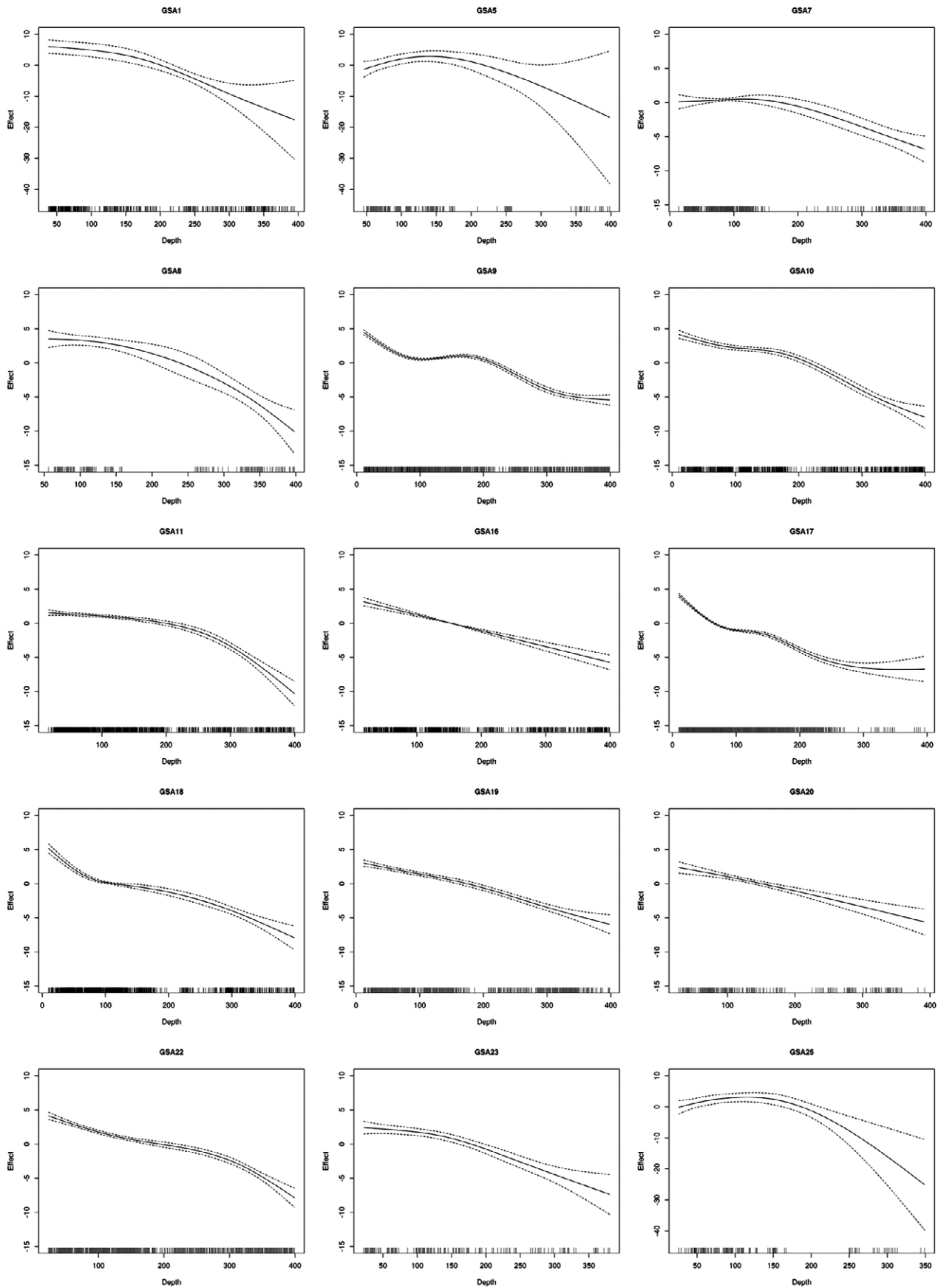


Fig. 3. – GAM-derived effect of depth (m) on the biomass index ( $\text{kg km}^{-2}$ ) of *M. barbatus*, by GSA. Zero lines indicate mean model estimates. Broken lines indicate two standard errors and the relative density of data points is shown by the “rug” on the x-axis.

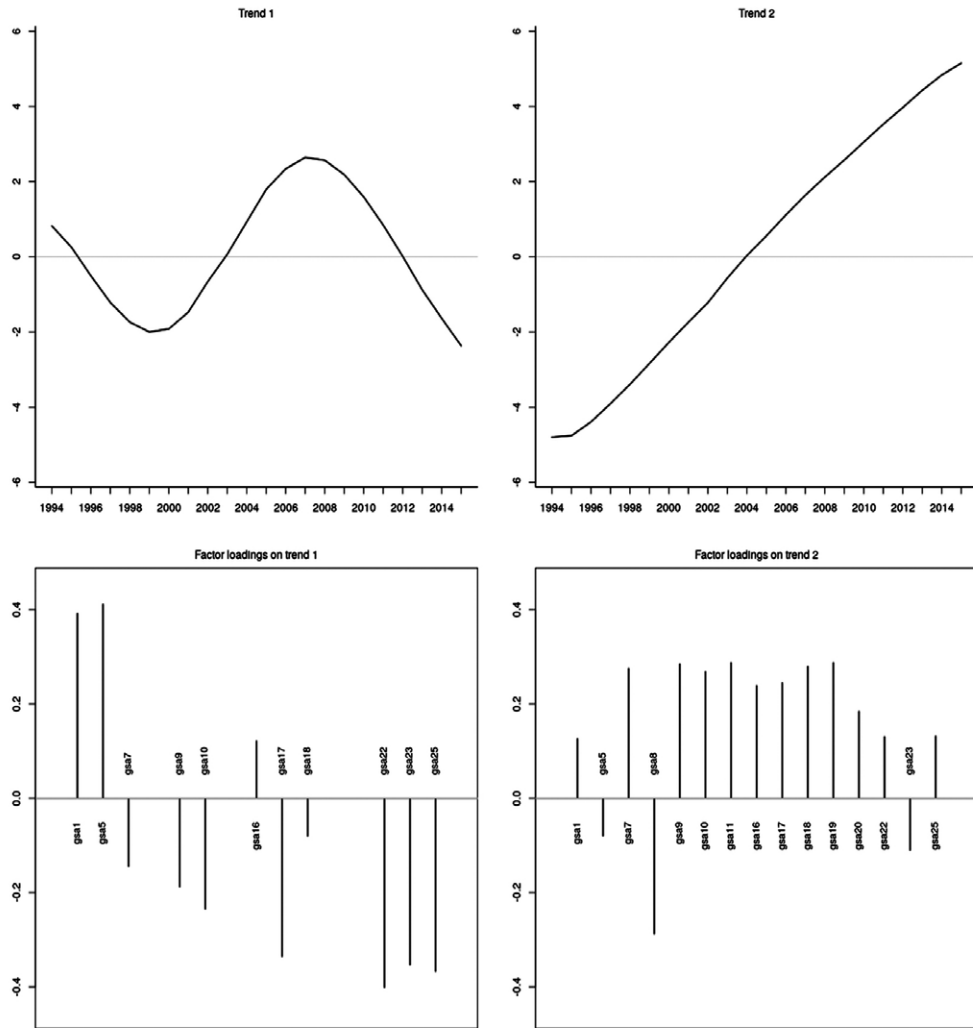


Fig. 4. – Common trends and factor loadings for the DFA model fitted to the *M. barbatus* standardized estimates obtained from the GAM models.

model with two CTs was considered the best solution. The first CT showed a pattern including a sequence of sharp decreases/increases. Specifically, biomass drops were observed up to 2000, followed by an increasing trend until 2008 and a decrease afterwards. (Fig. 4). The second CT showed a continuous increasing trend throughout the period examined. The fitted values suggested that most time series were fitted well to the model (Supplementary material Fig. S1). The factor loadings for the DFA model indicated which CT was related to which GSA time series (Fig. 4). The scores indicated roughly that the first CT was important for GSAs 1, 5, 22, 23 and 25, while the second was related to GSAs 7, 8, 9-11 and 18-20. GSAs 10 and 17 were influenced almost equally by both CTs (opposite sign for the first CT) but with low relevance, given the low scores (GSA 10 in particular).

Cluster analysis revealed two major GSA groups, each of them including minor subgroups (Fig. 5). All groups were delimited by the geographical position of the GSAs, i.e. the major groups separated eastern to western GSAs, while subgroups included nearby GSAs.

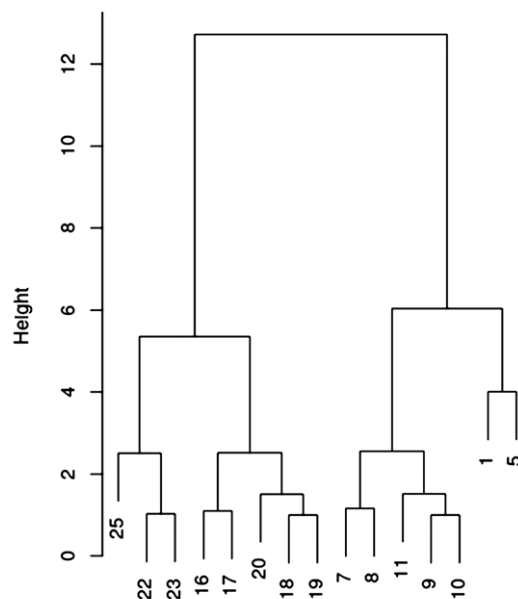


Fig. 5. – Cluster dendrogram of the hierarchical cluster analysis applied to the factor loadings estimated from the DFA for *M. barbatus*. The height of the vertical line indicates the Euclidean distance between GSAs.

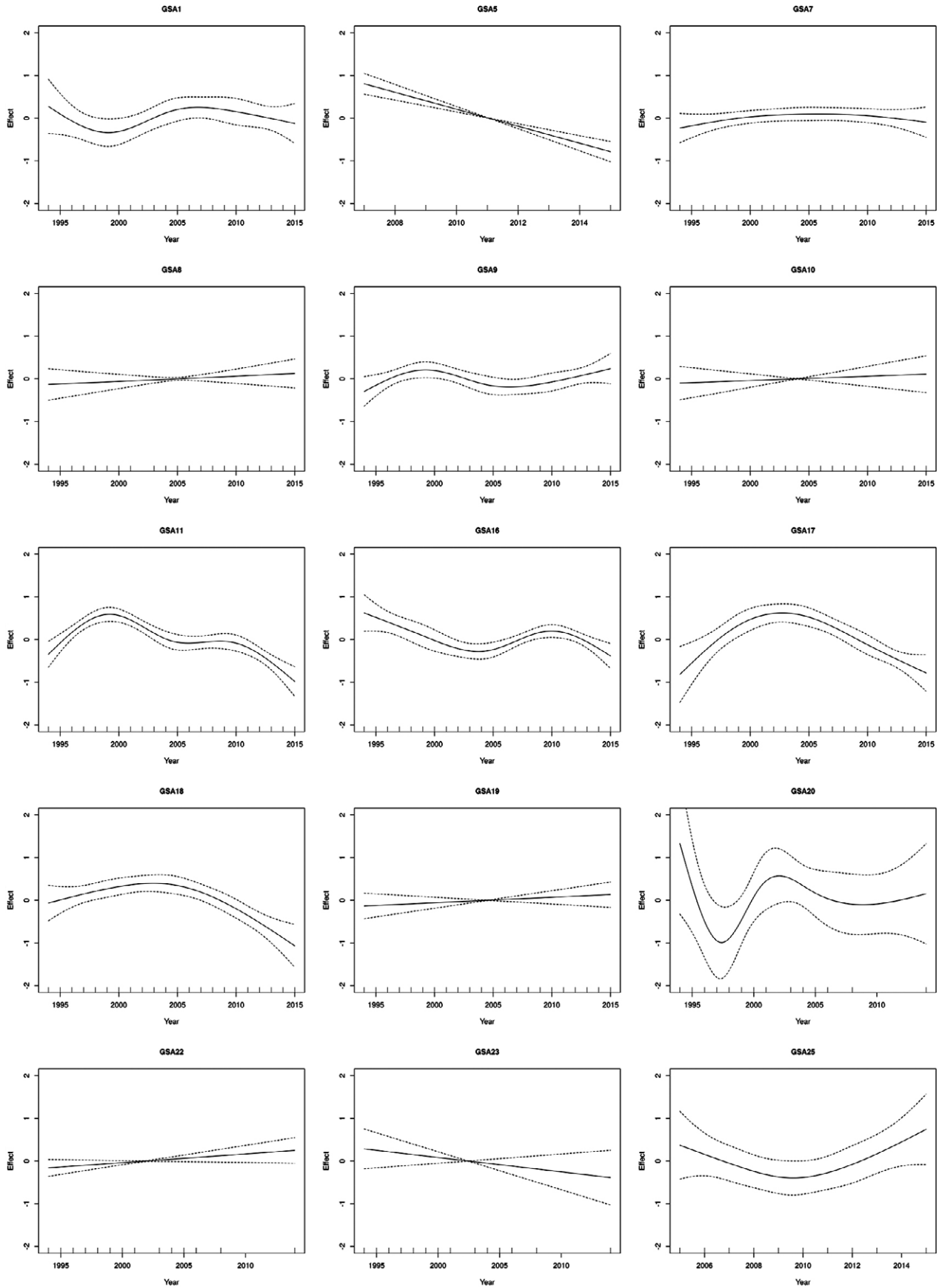


Fig. 6. – GAM-derived effect of year on the biomass index ( $\text{kg km}^{-2}$ ) of *M. surmuletus* by GSA. Zero lines indicate mean model estimates and broken lines indicate two standard errors. Statistical significance was found only in five GSAs (5, 11 and 16-18).

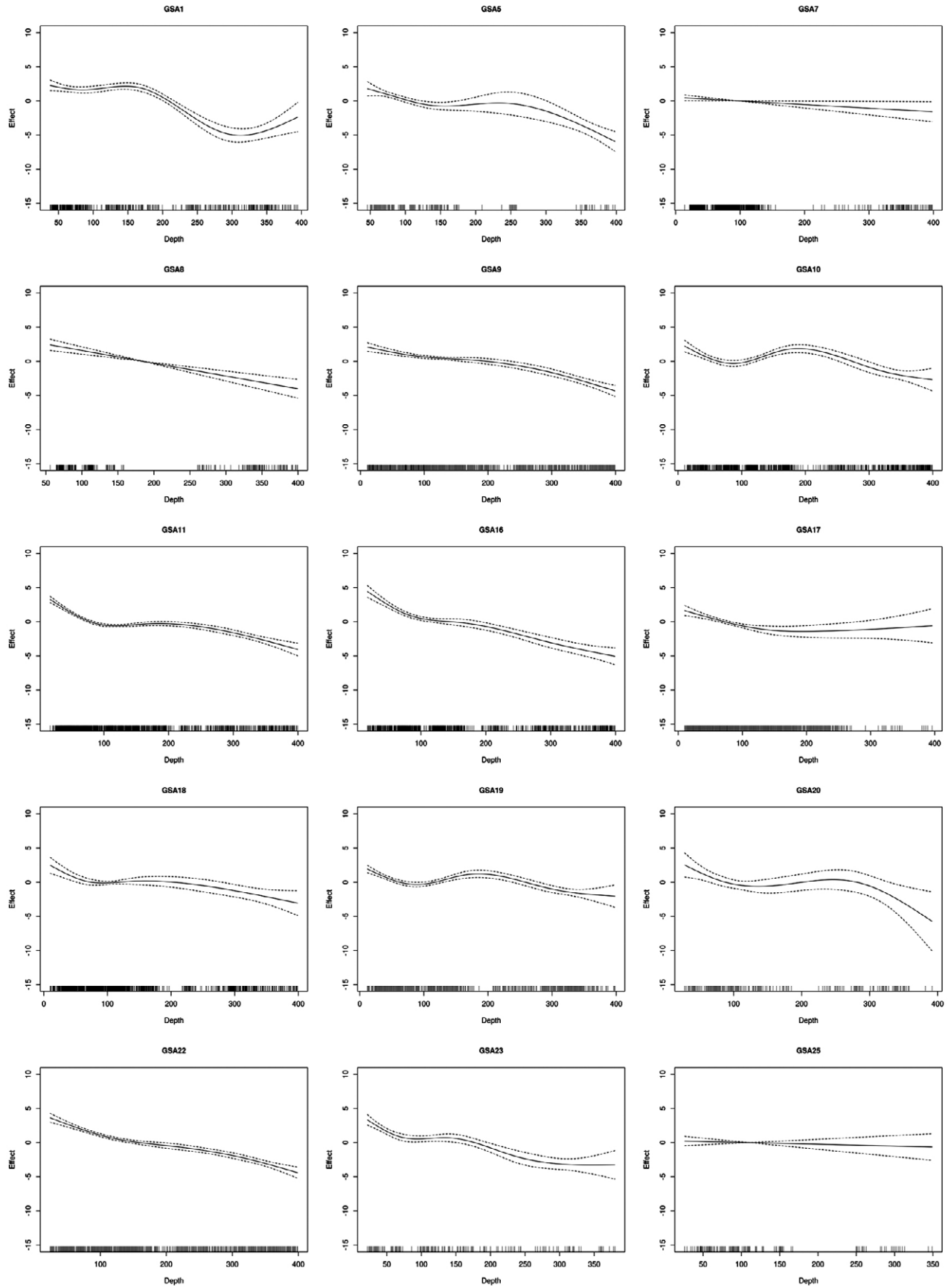


Fig. 7. – GAM-derived effect of depth (m) on the biomass index ( $\text{kg km}^{-2}$ ) of *M. surmuletus* by GSA. Zero lines indicate mean model estimates. Broken lines indicate two standard errors and the relative density of data points is shown by the “rug” on the x-axis.

Table 2. – Mean and standard error of biomass index estimates (kg km<sup>-2</sup>) for *M. surmuletus*, by GSA. The last column indicates the number of stations at depths of less than 400 m.

GSA	Mean	Std error	N
1 - Northern Alboran Sea	11.25	2.51	521
5 - Balearic Island	84.85	25.11	357
7 - Gulf of Lion	1.73	0.20	1288
8 - Corsica	11.83	2.31	305
9 - Ligurian and northern Tyrrhenian Seas	1.37	0.21	2081
10 - Southern and central Tyrrhenian Seas	0.42	0.09	1006
11 - Sardinia	13.97	1.21	1766
16 - Southern Sicily	8.82	0.85	1103
17 - Northern Adriatic Sea	0.44	0.05	3638
18 - Southern Adriatic Sea	0.89	0.11	1709
19 - Western Ionian Sea	2.21	0.36	884
20 - Eastern Ionian Sea	0.59	0.13	316
22 - Aegean Sea	11.27	2.00	1311
23 - Crete	16.60	4.58	217
25 - Cyprus	0.98	0.20	215

***M. surmuletus***

The highest values of mean standardized biomass (kg km<sup>-2</sup>) were observed in GSAs including islands, with the Balearics (GSA 5) having by far the highest rate (Table 2). Other GSAs with relatively high values were Crete (GSA 23), the Aegean Sea (GSA 22), Corsica (GSA 8) and Sardinia (GSA 11).

The GAM models applied explained in most cases more than 30% of the biomass variance, and depth and station position (longitude-latitude interactions) were

always significant. The effect of year was significant in only five of the GSAs (5, 11 and 16-18), located mostly in the central Mediterranean (Supplementary material Table S2). In these cases, a declining trend was observed in the latest years (Fig. 6). Generally, biomass was found to decrease progressively with depth, but in several GSAs this was more evident at depths below 250 to 300 m (Fig. 7).

DFA model fitting to the 15 time series was accomplished assuming 1 to 3 CTs. The AIC values for the one-, two- and three-CT models were 723.78, 712.84 and 718.15, respectively. Thus, the model with two CTs was considered the best solution. The first CT showed a continuous increasing pattern throughout the period examined, while the second was rather dome-shaped, with the peak in 2003-2004 (Fig. 8). The fitted values suggest that most time series were fitted well to the model (Supplementary material Fig. S2). The factor loadings scores indicate roughly that the first CT is more relevant for GSAs 8, 10, 19, 22 and 23 (opposite sign), while the second one is mostly related to GSAs 5, 7, 17 and 25 (opposite sign). GSAs 11, 16 and 18 are influenced almost equally by both CTs, while GSA 20 has very low factor loadings (not shown in Fig. 8) suggesting negligible relevance with the identified CTs.

Hierarchical cluster analysis applied on the factor loadings revealed two major groups, each of them in-

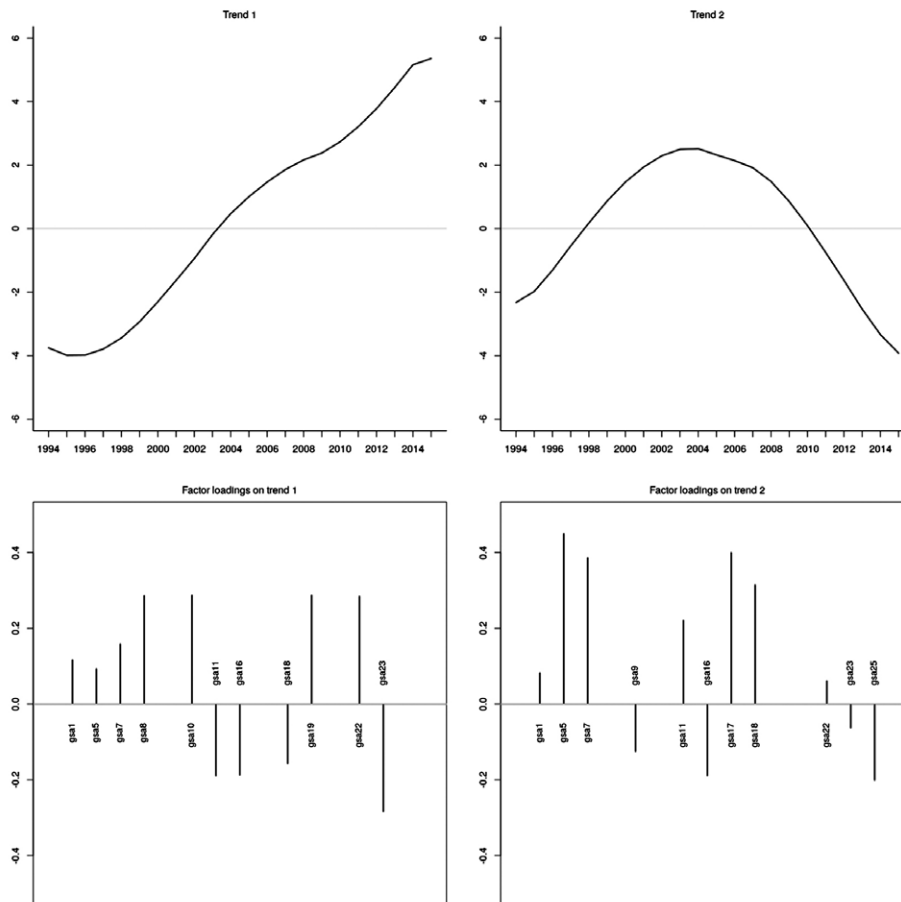


Fig. 8. – Common trends and factor loadings for the DFA model fitted to the *M. surmuletus* standardized estimates obtained from the GAM models.

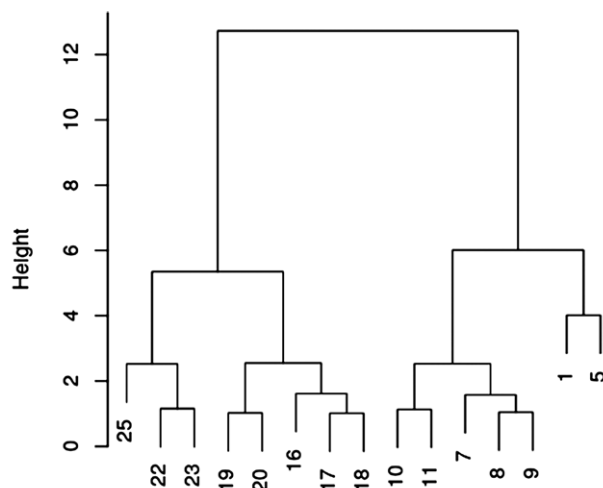


Fig. 9. – Cluster dendrogram of the hierarchical cluster analysis applied to the factor loadings estimated from the DFA for *M. surmuletus*. The height of the vertical line indicates the Euclidean distance between GSAs.

cluding minor subgroups (Fig. 9). Similarly to *M. barbatus*, all groups were delimited by the geographical position of the GSAs, i.e. the major groups separated eastern to western GSAs, while subgroups included nearby GSAs.

## DISCUSSION

The common sampling protocols followed by the MEDITS surveys give the opportunity of performing Mediterranean-wide studies of the species distribution patterns following harmonized analysis, which facilitates the detection of large-scale events. In the current work, the use of GAM techniques for computing standardized biomass rates removed effects that could bias nominal indexes (Hilborn and Walters 1992) and allowed direct comparisons among areas and identification of CTs. Utilizing a Tweedie distribution model, which has been reported to perform statistically better than a delta-type two-step model (Shono 2008), also allowed simultaneous analysis of zero and positive values and facilitated interpretation of the results.

As the MEDITS surveys are accomplished at the end or just after the reproduction period of red mullets, full recruitment of the newly born individuals to the surveyed fishing grounds cannot be traced. In fact, the MEDITS surveys are accomplished during the May–July period, while recruitment occurs from August to October (Suau and Vives 1957, Reñones et al. 1995). For this reason, the identification of spatio-temporal differences through the analysis of a biomass index was preferred, since such an index is less sensitive than one expressed in terms of numbers to spatio-temporal fluctuations owing to the irregular presence of recruits.

Our results indicate that biomass of both species shows clear declining trends after 150- to 200 m depth, and this decline is sharper in the case of *M. barbatus*. This finding is in line with previous studies suggesting that *M. surmuletus* has a wider bathymetric range than its congeneric species (Lombarte et al. 2000). In addition, it has been found that *M. barbatus* was more

abundant than *M. surmuletus* in all examined areas except the Balearic Islands, where the opposite situation occurs. However, the abundance of *M. surmuletus* may have been underestimated, owing to its preference for rough bottoms not always accessible to the bottom-trawl gear.

For both species, differences in the spatial distribution pattern can be attributed, at least to a certain extent, to the different biotic and abiotic conditions prevailing in each area. Past studies have suggested that certain geo-morphological and seafloor characteristics affect the distribution of red mullets. *M. surmuletus* prefers rough substrates and narrow continental shelves, while *M. barbatus* is more abundant on muddy bottoms and areas where the continental shelf becomes wider (Hureau 1986, Fischer et al. 1987, Lombarte et al. 2000). In addition, eco-morphological studies suggest the existence of adaptive morphological and anatomical characteristics that allow *M. barbatus* to exploit better than its congeneric species resources from muddy and turbid bottoms (Lombarte and Aguirre 1997). *M. surmuletus* seems to have more developed hearing sensitivity (Lombarte 1992, Aguirre and Lombarte 1999), which would give greater adaptation to relatively noisy environments, such as reefs or inshore waters.

Regarding temporal biomass patterns, increases were observed for *M. barbatus* from 2008 onward in several GSAs. Such increases are in line with recent assessment studies suggesting that several Mediterranean red mullet stocks are in healthy condition, or at least in much better situation than stocks of species inhabiting deeper waters (Vasilakopoulos et al. 2014, Tserpes et al. 2016, STECF 2016, Cardinale and Scarcella 2017). It is likely that the implementation of Council Regulation (EC) No 1967/2006, which introduced additional trawling prohibitions in coastal areas, has contributed to this increase (Tserpes et al. 2011).

Given that recruitment of both species mainly occurs at bottoms very close to the coast, at depths ranging from 10 to 50 m (Suau and Vives 1957, Levi et al. 2003), the establishment of satellite-based vessel monitoring systems through Council Regulation (EC) No 1224/2000 has also favoured such increases by discouraging illegal fishing operations in coastal areas. Furthermore, the mesh-size specifications introduced through the aforementioned regulation improved size selectivity of the bottom-trawl fishery by increasing the length at first capture of *M. barbatus* by 30% to 50% (Sala et al. 2015), thus contributing to overall biomass increases of the species, and most likely to the number of larger spawners.

Several past studies have identified a positive effect of female age/size on larva survival, concluding that the maternal effect on egg quality is very important for recruitment success (Trippel et al. 1997, Vallin and Nissling 2000, Nazari et al. 2009). In line with these findings, a recent study on the reproductive potential of *M. barbatus* in the southern Adriatic Sea showed that fish length was positively correlated with egg size and plasmatic concentration of vitellogenin, suggesting that survival rates of larvae coming from bigger/older females are higher than those hatched from eggs pro-

duced by smaller/younger individuals (Carbonara et al. 2015). Thus, it is expected that abundance increases of larger spawners, due to selectivity improvements, would lead to overall biomass increases of the species.

The temporal biomass pattern is different for *M. surmuletus*, which, showed stability in the majority of the GSAs, similarly to what has been reported in a past study that analysed a shorter time series of MEDITS data in various Mediterranean areas (Tserpes et al. 2002). Given that *M. surmuletus* also inhabits rough bottoms not exploited by trawlers but accessible to other fishing gears, it is likely that the aforementioned trawling prohibitions have less positive impact on it than on *M. barbatus*. In the Balearic Islands, the only area where *M. surmuletus* shows very clear decreasing trends throughout the period examined, the species is widely distributed in rocky and gravel bottoms, which predominate on the shelf of the archipelago, and it is an important target species for the fisheries operating in the area (Quetglas et al. 2012).

Apart from changes in the fisheries exploitation pattern, environmental changes may have favoured the increasing trends observed in certain areas. In the Aegean Sea for instance, increasing abundance trends for several demersal species have been partially attributed to recruitment increases owing to increased productivity (Tserpes and Peristeraki 2002). Certainly, the intensity of fishing activities always plays an important role, and this may explain why areas of low fishing pressure, such as GSA 23 (Crete), show relatively high abundances (Table 1) although they are characterized by low primary production (Peristeraki et al. 2017).

Levi et al. (2003), suggested that positive sea surface temperature (SST) anomalies (warmer waters than average) could enhance recruitment of *M. barbatus*, probably through a reduced upwelling regime, which—although it may involve lower productivity—would result in lower offshore transport of early fish stages, a key factor for the survival of juvenile stages. Maravelias et al. (2007) reported that red mullet abundance in the Aegean Sea (eastern Mediterranean) was consistently higher in areas with warmer waters near the seabed. Fiorentino et al. (2008) suggested that SST increases in the waters of northwestern Sicily during the pre-recruitment phase of red mullet could have a positive effect on the stock, contributing to the benefits derived from trawling bans. Under such scenarios, the warming trends of the Mediterranean waters (e.g. Nykjaer 2009, Vargas-Yáñez et al. 2008) may have favoured the recruitment of *M. barbatus* in several areas. Although there is a lack of relevant physiological studies, the differences in the spatial distribution pattern of the species (Kaschner et al. 2016) suggest that *M. barbatus* is more thermophilic than its congeneric. Consequently, sea-water warming may have contributed more to population increases of *M. barbatus* than to those of *M. surmuletus*.

Although it is reasonable to assume that the combined effects of fishing and environmental conditions determine species abundance variations, the relative importance of each component may vary among areas. Examination of stock dynamics in areas with different

environmental characteristics and various levels of fishing pressure would help to clarify the magnitude of each component, as well as the way they interact (Rouyer et al. 2008).

DFA revealed similarities among neighbouring GSAs in terms of temporal abundance trends, and the subsequent cluster analysis identified two major GSA groups corresponding to the eastern and western part of the Mediterranean basin (Figs 5 and 9). As both species have a pelagic larval stage, larval dispersal may, at least to a certain extent, explain similarities in abundance trends among nearby areas. In general, the spatial connectivity among fish populations has been traditionally attributed to larval dispersal and adult movements (Grüss et al. 2011). Given the low mobility of red mullets and the fact that their eggs and larvae are pelagic, with larvae being able to remain 25–35 days in the water column until they find a suitable habitat to settle (Macpherson and Raventos 2006), it can be assumed that larval dispersal and survival determined by environmental conditions are of critical importance in the context of the spatial biomass differences observed in the current study. In line with this, Gargano et al. (2017) reported that the connectivity between *M. barbatus* population sub-units inhabiting the European and African shelves of the Strait of Sicily was low, and high quantities of larvae were transported outside the study area. Based on the biological features of the species and the patterns of the sea-water currents, the authors suggested that larvae and pre-recruits lost from the Strait of Sicily can reach suitable coastal areas to recruit even far from their natal area, supporting the existence of a meta-population structure, sensu Kerr and Goethel (2014), of red mullet in the Strait of Sicily and the adjacent areas.

Genetic studies give a more complex pattern regarding spatial connectivity of red mullet populations in the Mediterranean. Maggio et al. (2009), working on six microsatellite loci of *M. barbatus* from 14 different sites of the central Mediterranean, reported the isolation of the Adriatic samples and a weaker substructuring of the populations in the Gulf of Lions, the Tyrrhenian Sea, the Strait of Sicily and the Ionian Sea. Recently, Matić-Skoko et al. (2018) working on 13 microsatellite loci from 15 Mediterranean sites found differences in the genotype of *M. barbatus* inhabiting the eastern and western coast of the southern Adriatic Sea, while no differences were reported for the northern and middle Adriatic populations. Surprisingly, no gene barrier was observed between the Balearic Sea and the eastern Mediterranean, while the Tyrrhenian Sea specimens were grouped together with the northern and middle Adriatic populations. In the case of *M. surmuletus* a lower level of genetic heterogeneity was found between populations. The authors evidenced a clear sign of genetic bottleneck in both species that was attributed to demographic changes caused by a combination of high fishing pressure, habitat fragmentation and naturally occurring fluctuations in population size.

Discrepancies between population dynamics and genetic studies in questions related to the spatial con-

nectivity of populations are most likely due to the different temporal scale underlying the two approaches. While results of genetic studies reflect dynamics at the evolutionary scale, classical population dynamics depict variations at the ecological scale, which is shorter and limited to rather recent events.

Our findings regarding spatial association could be used for management purposes to assist the identification of population units that behave as a single stock with the same population dynamics (Cope and Punt 2009). Spatial connectivity, however, depends on numerous parameters and interdisciplinary studies are necessary to provide robust conclusions on the structure of the stocks and support the rational management of fishery resources.

## ACKNOWLEDGEMENTS

The authors would like to thank Dr Antoni Quetglas for helpful comments on an earlier version of the manuscript.

## REFERENCES

- Aguirre H., Lombarte A. 1999. Ecomorphologic comparisons of sagittae in *Mullus barbatus* and *M. surmuletus*. *J. Fish Biol.* 55: 105-114.  
<https://doi.org/10.1111/j.1095-8649.1999.tb00660.x>
- Bertrand J.A., Gil de Sola L., Papaconstantinou C., et al. 2002. The general specifications of the MEDITS surveys. *Sci. Mar.* 66 (Suppl. 2): 9-17.
- Carbonara P., Intini S., Modugno E., et al. 2015. Reproductive biology characteristics of red mullet (*Mullus barbatus* L., 1758) in Southern Adriatic Sea and management implications. *Aquat. Living Resour.* 28: 21-31.  
<https://doi.org/10.1051/alr/2015005>
- Cardinale M., Scarcella G. 2017. Mediterranean Sea: A Failure of the European Fisheries Management System. *Front. Mar. Sci.* 4: 72.  
<https://doi.org/10.3389/fmars.2017.00072>
- Cope J.M., Punt A.E. 2009. Drawing the lines: resolving fishery management units with simple fisheries data. *Can. J. Fish. Aquat. Sci.* 66: 1256-1273.  
<https://doi.org/10.1139/F09-084>
- Farrugio H., Oliver P., Biagi F. 1993. An overview of the history, knowledge, recent and future research trends in Mediterranean fisheries. *Sci. Mar.* 57: 105-119.
- Fiorentino F., Badalamenti F., D'Anna G., et al. 2008. Changes in spawning-stock structure and recruitment pattern of red mullet, *Mullus barbatus*, after a trawl ban in the Gulf of Castellammare (central Mediterranean Sea). *ICES J. Mar. Sci.* 65: 1175-1183.  
<https://doi.org/10.1093/icesjms/fsn104>
- Fischer W., Bauchot M.L., Schneider M. 1987. Fiches FAO d'identification des espèces pour les besoins de la pêche. (Révision 1). Méditerranée et Mer Noire. Zone de pêche 37. 2. Vertébrés. Publication préparée par la FAO (Project GCP/INT/422/EEC). Rome, FAO: 761-1530.
- Foster S.D., Bravington M.V. 2013. A Poisson-Gamma model for analysis of ecological non-negative continuous data. *Envir. Ecol. Stat.* 20: 533-552.  
<https://doi.org/10.1007/s10651-012-0233-0>
- Gargano F., Garofalo G., Fiorentino F. 2017. Exploring connectivity between spawning and nursery areas of *Mullus barbatus* (L., 1758) in the Mediterranean through a dispersal model. *Fish. Oceanogr.* 26: 476-497.  
<https://doi.org/10.1111/fog.12210>
- Grüss A., Kaplan D.M., Hart D.R. 2011. Relative impacts of adult movement, larval dispersal and harvester movement on the effectiveness of reserve networks. *PLoS ONE* 6: e19960.  
<https://doi.org/10.1371/journal.pone.0019960>
- Hastie T.J., Tibshirani R.J. 1990. Generalized additive models. Chapman and Hall, London, 352 pp.
- Holmes E.E., Ward E.J., Wills K. 2012. MARSS: Multivariate Autoregressive State-space Models for Analyzing Time-series Data. *The R Journal* 4: 11-19.
- Hilborn R., Walters C.J. 1992. Quantitative fisheries stock assessment. Chapman and Hall, London, 570 pp.
- Hureau J.C. 1986. Mullidae. In: Whitehead P.J.P., Bauchot M.L., et al. (eds), Fishes of the North-eastern Atlantic and the Mediterranean, UNESCO, Paris. Vol. II, pp. 877-882.
- Kaschner K., Kesner-Reyes K., Garilao C., et al. 2016. AquaMaps: Predicted range maps for aquatic species. World wide web electronic publication, <http://www.aquamaps.org>, Version 08/2016.
- Kerr L.A., Goethel D.R. 2014. Simulation modeling as a tool for synthesis of stock identification information. In: Cadrin S.X., Kerr L.A., Mariani S. (eds), Stock Identification Methods. Applications in Fishery Science, Elsevier Academic Press (2nd ed.), pp. 502-533.
- Lecomte J-B., Benoit H.P., Ancelet S., et al. 2013. Compound Poisson-gamma vs. delta-gamma to handle zero-inflated continuous data under a variable sampling volume. *Methods Ecol. Evol.* 4: 1159-1166.  
<https://doi.org/10.1111/2041-210X.12122>
- Levi D., Andreoli M.G., Bonanno A., et al. 2003. Embedding sea surface temperature anomalies into the stock recruitment relationship of red mullet (*Mullus barbatus* L. 1758) in the Strait of Sicily. *Sci. Mar.* 67(Suppl. 1): 259-268.  
<https://doi.org/10.3989/scimar.2003.67s1259>
- Lombarte A. 1992. Changes in otolith area: sensory area ratio with body size and depth. *Environ. Biol. Fishes* 33: 405-410.  
<https://doi.org/10.1007/BF00010955>
- Lombarte A., Aguirre H. 1997. Quantitative differences in the chemoreceptor systems in the barbells of two species of Mullidae (*Mullus surmuletus* and *M. barbatus*) with different bottom habitats. *Mar. Ecol. Prog. Ser.* 150: 57-64.
- Lombarte A., Recasens L., Gonzalez M., et al. 2000. Spatial segregation of two species of Mullidae (*Mullus surmuletus* and *M. barbatus*) in relation to habitat. *Mar. Ecol. Prog. Ser.* 206: 239-249.
- Machias A., Somarakis S., Tsimenides N. 1998. Bathymetric distribution and movements of red mullet *Mullus surmuletus*. *Mar. Ecol. Prog. Ser.* 166: 247-257.
- Macpherson E., Raventos N. 2006. Relationship between pelagic larval duration and geographic distribution of Mediterranean littoral fishes. *Mar. Ecol. Prog. Ser.* 327: 257-265.  
<https://doi.org/10.3354/meps327257>
- Maggio T., Brutto S.L., Garioia F., et al. 2009. Microsatellite analysis of red mullet *Mullus barbatus* (Perciformes, Mullidae) reveals the isolation of the Adriatic Basin in the Mediterranean Sea. *ICES J. Mar. Sci.* 66: 1883-1891.  
<https://doi.org/10.1093/icesjms/fsp160>
- Maravelias C.D., Tsitsika V., Papaconstantinou C. 2007. Environmental influences on the spatial distribution of European hake (*Merluccius merluccius*) and red mullet (*Mullus barbatus*) in the Mediterranean. *Ecol. Res.* 22: 678-685.  
<https://doi.org/10.1007/s11284-006-0309-0>
- Matić-Skoko S., Šegvić-Bubić T., Mandić I., et al. 2018. Evidence of subtle genetic structure in the sympatric species *Mullus barbatus* and *Mullus surmuletus* (Linnaeus, 1758) in the Mediterranean Sea. *Sci. Rep.* 8: 676.  
<https://doi.org/10.1038/s41598-017-18503-7>
- Nazari R.M., Sohrabnejad M., Ghomi M.R., et al. 2009. Correlation between egg size and dependent variables related to larval stage in Persian sturgeon *Acipenser persicus*. *Mar. Freshw. Behav. Physiol.* 42: 147-155.  
<https://doi.org/10.1080/10236240902846796>
- Nykjaer L. 2009. Mediterranean Sea surface warming 1985-2006. *Clim. Res.* 39: 11-17.
- Papaconstantinou C., Farrugio H. 2000. Fisheries in the Mediterranean. *Medit. Mar. Sci.* 1: 5-18.
- Peristeraki P., Tserpes G., Lampadariou N., et al. 2017. Comparing demersal megafaunal species diversity along the depth gradient within the South Aegean and Cretan Seas (Eastern Mediterranean). *PLoS ONE* 12: e0184241.  
<https://doi.org/10.1371/journal.pone.0184241>
- Quetglas A., Guijarro B., Ordines F., et al. 2012. Stock boundaries for fisheries assessment and management in the Mediterranean: the Balearic Islands as a case study. *Sci. Mar.* 76: 17-28.  
<https://doi.org/10.3989/scimar.2012.76n1017>
- Relini G., Bertrand J., Zamboni A. 1999. Synthesis of the knowledge on bottom fishery resources in Central Mediterranean (Italy and Corsica). *Biol. Mar. Medit.* 6 (Suppl.1): 276-299.
- Reñones O., Massutí E., Morales-Nin B. 1995. Life history of the

- red mullet *Mullus surmuletus* from the bottom-trawl fishery off the Island of Majorca (north-west Mediterranean). *Mar. Biol.* 123: 411-419.
- Rouyer T., Fromentin J.-M., Menard F., et al. 2008. Complex interplays among population dynamics, environmental forcing, and exploitation in fisheries. *PNAS* 105: 5420-5425. <https://doi.org/10.1073/pnas.0709034105>
- Sala A., Lucchetti A., Perdicchizzi A., et al. 2015. Is square-mesh better selective than larger mesh? A perspective on the management for Mediterranean trawl fisheries. *Fish. Res.* 161: 182-190. <https://doi.org/10.1016/j.fishres.2014.07.011>
- Shono H. 2008. Application of the Tweedie Distribution to Zero-catch Data in CPUE Analysis. *Fish. Res.* 93: 154-162. <https://doi.org/10.1016/j.fishres.2008.03.006>
- Scientific, Technical and Economic Committee for Fisheries (STECF). 2016. Mediterranean assessments part 2 (STECF-16-08). Publications Office of the European Union, Luxembourg, EUR 27758 EN, JRC 101548, 483 pp.
- Spedicato M.T., Massutí E., Mérigot B. et al. 2019. The MEDITS trawl survey specifications in an ecosystem approach to fishery management. *Sci. Mar.* 83S1: 9-20. <https://doi.org/10.3989/scimar.04915.11X>
- Suau P., Vives F. 1957. Contribución al estudio del salmonete de fango (*Mullus barbatus* L.) del Mediterráneo occidental. *Invest. Pesq.* 9: 97-118.
- Trippel E.A., Kjesbu O.S., Solemdal P. 1997. Effects of adult age and size structure on reproductive output in marine fishes. In: Chambers R.C., Trippel E.A. (eds), *Early Life History and Recruitment in Fish populations*. Chapman and Hall, New York, pp. 31-62.
- Tserpes G., Peristeraki P. 2002. Trends in the abundance of demersal species in the southern Aegean Sea. *Sci. Mar.* 66 (Suppl. 2): 243-252.
- Tserpes G., Peristeraki P., Potamias G., et al. 1999. Species distribution in the southern Aegean Sea based on bottom-trawl surveys. *Aquat. Liv. Res.* 12: 167-175.
- Tserpes G., Fiorentino F., Levi D., et al. 2002. Distribution of *Mullus barbatus* and *M. surmuletus* (Osteichthyes: Perciformes) in the Mediterranean continental shelf: implications for management. *Sci. Mar.* 66(Suppl. 2): 39-54.
- Tserpes G., Tzanatos E., Peristeraki P. 2011. Spatial management of the Mediterranean bottom-trawl fisheries; the case of the southern Aegean Sea. *Hydrobiologia* 670: 267-274. <https://doi.org/10.1007/s10750-011-0667-7>
- Tserpes G., Nikolioudakis N., Maravelias C., et al. 2016. Viability and Management Targets of Mediterranean Demersal Fisheries: The Case of the Aegean Sea. *Plos ONE* 11: e0168694. <https://doi.org/10.1371/journal.pone.0168694>
- Vallin L., Nissling A. 2000. Maternal effects on egg size and egg buoyancy of the Baltic Cod, *Gadus morhua*; implications for stock structure effects on recruitment. *Fish. Res.* 49: 21-37.
- Vargas-Yáñez M., García M.J., Salat, J., et al. 2008. Warming trends and decadal variability in the Western Mediterranean shelf. *Glob. Plan. Change* 63: 177-184. <https://doi.org/10.1016/j.gloplacha.2007.09.001>
- Vasilakopoulos P., Maravelias C.D., Tserpes G. 2014. The Alarming Decline of Mediterranean Fish Stocks. *Curr. Biol.* 24: 1643-1648. <https://doi.org/10.1016/j.cub.2014.05.070>
- Wood S.N. 2003. Thin plate regression splines. *J. R. Stat. Soc. Ser. B (Statistical Methodology)* 65: 95-114.
- Wood S.N. 2006. *Generalized Additive Models: An introduction with R*. Chapman and Hall/CRC, Florida, 391 pp. <https://doi.org/10.1201/9781420010404>
- Zuur A.F., Fryer R.J., Jolliffe I.T., et al. 2003. Estimating common trends in multivariate time series using dynamic factor analysis. *Environmetrics* 14: 665-685.

## SUPPLEMENTARY MATERIAL

The following supplementary material is available through the online version of this article and at the following link: <http://scimar.icm.csic.es/scimar/supplm/sm04888esm.pdf>

Fig. S1. – Fitted values (line) and standardized biomass indexes of *M. barbatus* by year and GSA.

Fig. S2. – Fitted values (line) and standardized biomass indexes of *M. surmuletus* by year and GSA.

Table S1. – Analysis of deviance tables for the GAM models applied on *M. barbatus* biomass indexes in the different GSAs.

Table S2. – Analysis of deviance tables for the GAM models applied on *M. surmuletus* biomass indexes in the different GSAs.

*Mediterranean demersal resources and ecosystems:  
25 years of MEDITS trawl surveys*  
M.T. Spedicato, G. Tserpes, B. Mérigot and  
E. Massutí (eds)

SCIENTIA MARINA 83S1  
December 2019, S1-S4, Barcelona (Spain)  
ISSN-L: 0214-8358

## **Distribution and spatio-temporal biomass trends of red mullets across the Mediterranean**

George Tserpes, Enric Massuti, Fabio Fiorentino, Maria Teresa Facchini, Claudio Viva, Angélique Jadaud, Aleksandar Joksimovic, Paola Pesci, Corrado Piccinetti, Letizia Sion, Ioannis Thasitis, Nedo Vrgoc

Supplementary material

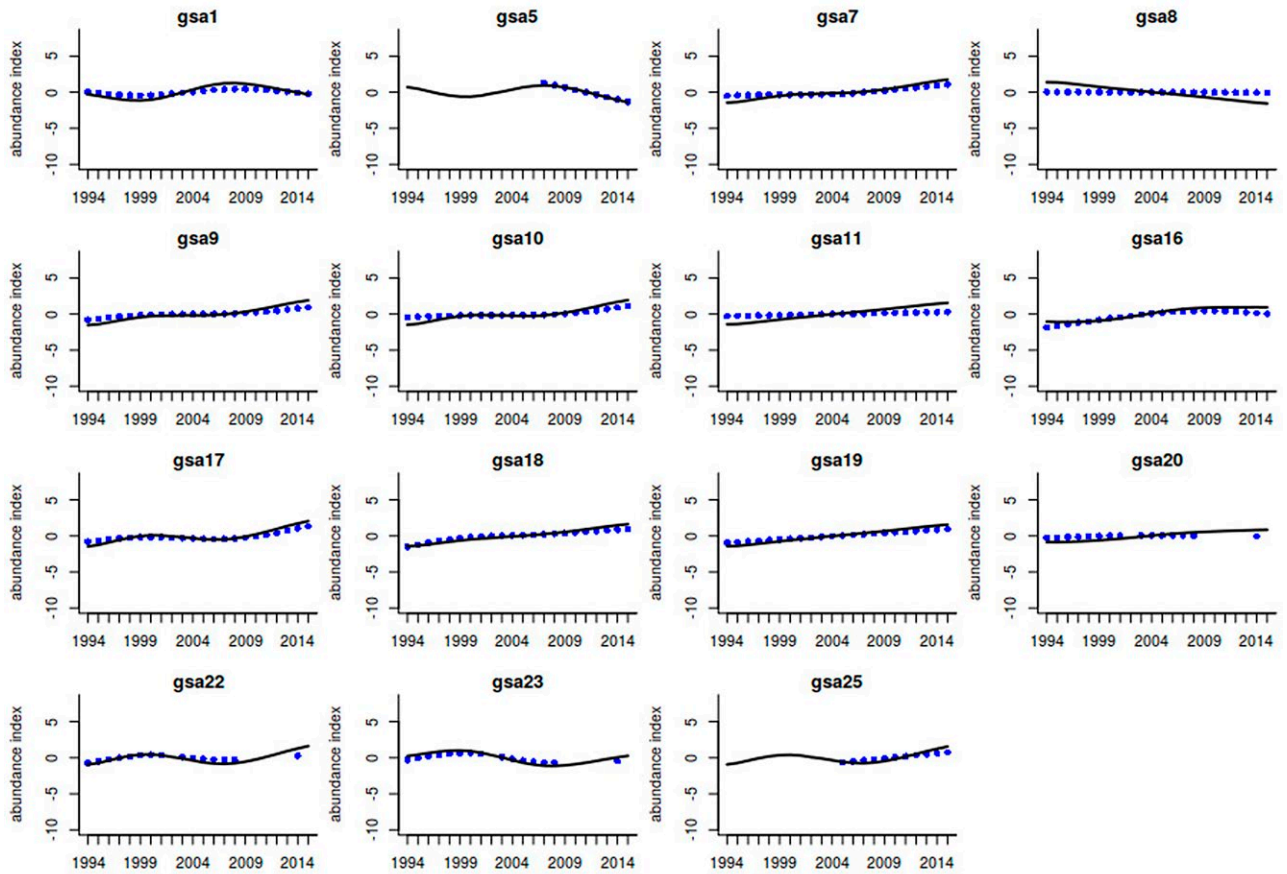


Fig. S1. – Fitted values (line) and standardized biomass indexes of *M. barbatus* by year and GSA.

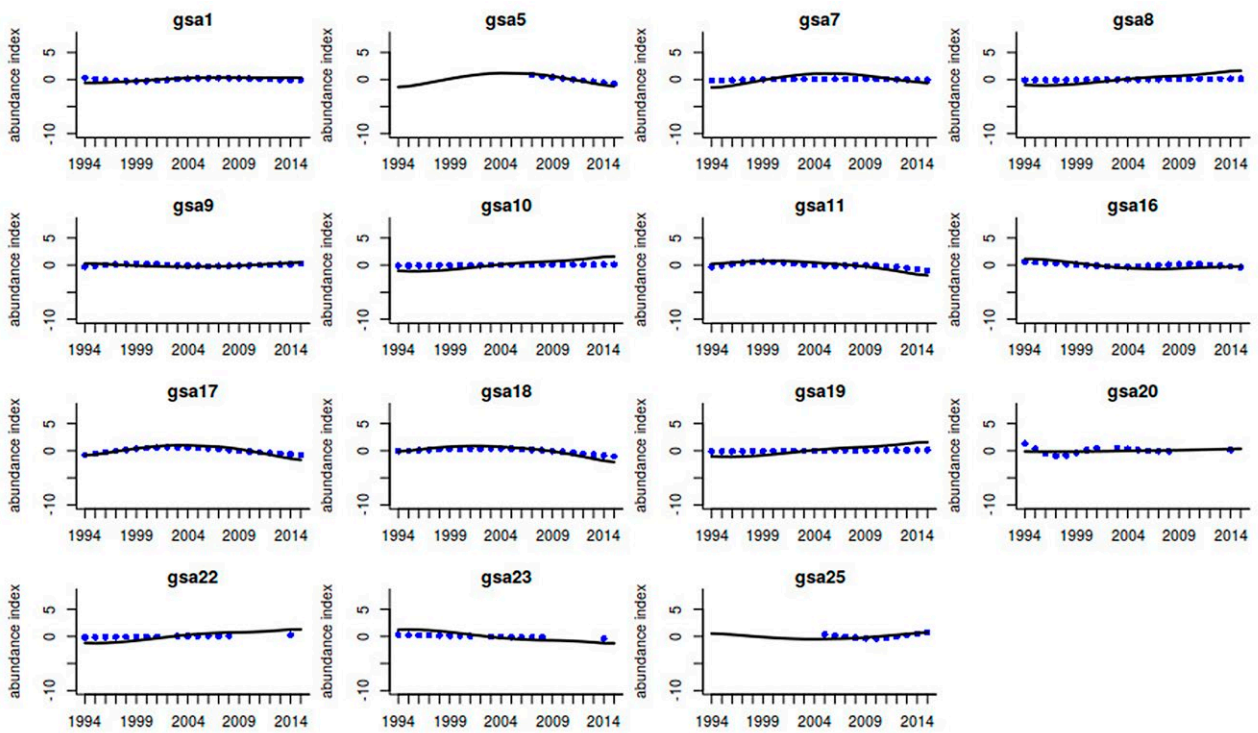


Fig. S2. – Fitted values (line) and standardized biomass indexes of *M. surmuletus* by year and GSA.

Table S1. – Analysis of deviance tables for the GAM models applied on *M. barbatus* biomass indexes in the different GSAs.

	edf	Ref.df	F	p-value
<b>GSA 1</b>				
s(Year)	3.335245	3.752963	5.135572	1.19E-03
s(Depth)	2.710464	3.001904	28.740873	1.70E-17
s(Lat,Lon)	17.865338	20.96536	17.162887	1.10E-54
Deviance explained = 0.7800034				
<b>GSA 5</b>				
s(Year)	1.000741	1.001481	43.833976	1.30E-10
s(Depth)	3.028411	3.445171	4.193971	3.37E-03
s(Lat,Lon)	21.549188	24.35983	6.707591	6.52E-19
Deviance explained = 0.6758651				
<b>GSA 7</b>				
s(Year)	3.099836	3.579545	54.83064	2.00E-37
s(Depth)	2.997409	3.508917	21.02387	7.23E-15
s(Lat,Lon)	27.572921	28.78585	40.85497	1.74E-207
Deviance explained = 0.5978377				
<b>GSA 8</b>				
s(Year)	1.001059	1.002107	0.05421135	8.16E-01
s(Depth)	2.599163	2.889314	30.30880747	1.14E-16
s(Lat,Lon)	9.766334	12.059621	4.36137273	2.24E-06
Deviance explained = 0.5626815				
<b>GSA 9</b>				
s(Year)	3.574405	3.892615	61.44117	1.65E-47
s(Depth)	3.980383	3.999239	279.18863	3.34E-223
s(Lat,Lon)	26.634597	28.517179	48.93436	3.39E-253
Deviance explained = 0.6498317				
<b>GSA 10</b>				
s(Year)	3.222359	3.670948	21.64876	1.35E-15
s(Depth)	3.681666	3.924182	89.52428	5.02E-68
s(Lat,Lon)	24.437275	27.153119	24.41404	2.14E-109
Deviance explained = 0.6864137				
<b>GSA 11</b>				
s(Year)	1.01524	1.030278	13.008963	2.83E-04
s(Depth)	3.732737	3.950188	72.190412	1.91E-56
s(Lat,Lon)	22.557447	26.543793	9.877832	9.60E-38
Deviance explained = 0.3302203				
<b>GSA 16</b>				
s(Year)	3.11864	3.582447	24.32054	4.98E-17
s(Depth)	1.003078	1.005674	113.32434	2.05E-25
s(Lat,Lon)	27.339479	28.613174	24.29931	3.43E-115
Deviance explained = 0.5748771				
<b>GSA 17</b>				
s(Year)	3.864937	3.988148	168.64287	1.63E-137
s(Depth)	3.968186	3.999094	219.05383	1.09E-179
s(Lat,Lon)	28.050589	28.939412	89.60738	0.00E+00
Deviance explained = 0.4526162				
<b>GSA 18</b>				
s(Year)	3.460161	3.831484	47.86305	5.14E-36
s(Depth)	3.885355	3.983931	106.80989	5.82E-77
s(Lat,Lon)	25.957258	28.255278	33.84446	2.89E-168
Deviance explained = 0.5904676				
<b>GSA 19</b>				
s(Year)	1.011616	1.022971	96.49018	4.71E-22
s(Depth)	2.690363	3.149898	79.29041	1.55E-48
s(Lat,Lon)	19.635589	23.297799	13.64767	6.04E-48
Deviance explained = 0.6149736				
<b>GSA 20</b>				
s(Year)	1.798056	2.189174	0.7464399	4.25E-01
s(Depth)	1.535974	1.768087	25.7361036	4.93E-08
s(Lat,Lon)	19.050257	22.93218	7.1640323	2.06E-19
Deviance explained = 0.6105294				
<b>GSA 22</b>				
s(Year)	3.477106	3.812682	7.171149	1.22E-05
s(Depth)	3.587654	3.886194	115.572978	3.84E-87
s(Lat,Lon)	26.246697	28.461454	15.377633	5.19E-68
Deviance explained = 0.5178125				
<b>GSA 23</b>				
s(Year)	3.140406	3.542358	4.755734	1.51E-03
s(Depth)	2.664722	3.147146	17.920273	8.72E-11
s(Lat,Lon)	6.105404	7.537994	4.73422	3.86E-05
Deviance explained = 0.5691011				
<b>GSA 25</b>				
s(Year)	1.000722	1.001432	8.850662	3.27E-03
s(Depth)	3.381659	3.737661	6.345404	8.35E-05
s(Lat,Lon)	11.436353	14.364692	3.914098	5.27E-06
Deviance explained = 0.4023809				

Table S2. – Analysis of deviance tables for the GAM models applied on *M. surmuletus* biomass indexes in the different GSAs.

	edf	Ref.df	F	p-value
<b>GSA 1</b>				
s(Year)	3.161466	3.629141	2.07928	2.32E-01
s(Depth)	3.868186	3.98051	28.542862	1.50E-21
s(Lat,Lon)	23.300676	26.662747	8.202271	1.06E-27
Deviance explained = 0.52453				
<b>GSA 5</b>				
s(Year)	1.001305	1.002608	43.80645	1.33E-10
s(Depth)	3.23774	3.575252	13.50772	1.74E-09
s(Lat,Lon)	26.210841	28.260532	10.32969	2.11E-37
Deviance explained = 0.5888375				
<b>GSA 7</b>				
s(Year)	1.913384	2.352321	1.025882	3.75E-01
s(Depth)	1.001219	1.002273	4.671017	3.06E-02
s(Lat,Lon)	24.719079	27.759875	16.693983	2.60E-73
Deviance explained = 0.5362836				
<b>GSA 8</b>				
s(Year)	1.0194	1.038332	0.5450814	4.76E-01
s(Depth)	1.00039	1.000631	34.4748563	1.11E-08
s(Lat,Lon)	11.17189	13.793766	5.343227	4.52E-09
Deviance explained = 0.4565079				
<b>GSA 9</b>				
s(Year)	3.287673	3.720515	2.944202	8.45E-02
s(Depth)	3.413051	3.807052	40.166843	1.43E-30
s(Lat,Lon)	24.001003	27.409868	20.692748	6.40E-95
Deviance explained = 0.3869566				
<b>GSA 10</b>				
s(Year)	1.000442	1.000882	0.2597142	6.11E-01
s(Depth)	3.84244	3.981262	15.9082461	2.07E-12
s(Lat,Lon)	5.622278	7.456302	5.3499085	3.29E-06
Deviance explained = 0.2864568				
<b>GSA 11</b>				
s(Year)	3.794239	3.973805	17.73862	4.06E-14
s(Depth)	3.91863	3.995226	62.47487	6.58E-50
s(Lat,Lon)	27.32056	28.811043	13.39936	9.78E-60
Deviance explained = 0.3128502				
<b>GSA 16</b>				
s(Year)	3.561823	3.886183	5.110776	2.94E-04
s(Depth)	3.748586	3.938694	34.527482	2.47E-26
s(Lat,Lon)	26.84692	28.60003	19.482595	1.46E-89
Deviance explained = 0.526563				
<b>GSA 17</b>				
s(Year)	3.129921	3.607009	11.206399	4.27E-08
s(Depth)	2.914772	3.412236	6.499741	1.25E-04
s(Lat,Lon)	23.541768	27.193338	7.783097	1.63E-29
Deviance explained = 0.2561995				
<b>GSA 18</b>				
s(Year)	2.745708	3.267287	7.56255	3.25E-05
s(Depth)	3.661944	3.879318	10.349626	4.36E-06
s(Lat,Lon)	20.472029	24.791741	8.649972	3.18E-30
Deviance explained = 0.2979741				
<b>GSA 19</b>				
s(Year)	1.001017	1.002028	0.7970839	3.72E-01
s(Depth)	3.844075	3.977881	19.7762281	2.45E-15
s(Lat,Lon)	7.482555	9.716561	6.4734054	2.06E-09
Deviance explained = 0.2618247				
<b>GSA 20</b>				
s(Year)	3.611608	3.883158	2.078063	0.142948241
s(Depth)	3.287364	3.664828	3.593405	0.008274185
s(Lat,Lon)	11.681975	15.317132	2.305099	0.003812417
Deviance explained = 0.4412766				
<b>GSA 22</b>				
s(Year)	1.011593	1.023049	2.631118	1.02E-01
s(Depth)	3.38738	3.779948	74.462578	9.72E-54
s(Lat,Lon)	25.884213	28.296685	20.082946	1.42E-92
Deviance explained = 0.4895741				
<b>GSA 23</b>				
s(Year)	1.000154	1.000307	1.4776095	2.25E-01
s(Depth)	3.712865	3.949588	25.9199559	6.47E-18
s(Lat,Lon)	2.000253	2.000504	0.8635837	4.23E-01
Deviance explained = 0.3599268				
<b>GSA 25</b>				
s(Year)	2.166719	2.623342	1.9102568	0.141361537
s(Depth)	1.000509	1.00093	0.4411788	0.507677568
s(Lat,Lon)	6.214226	8.203957	3.1211448	0.002454741
Deviance explained = 0.2561293				